Repeated Index Modulation with Coordinate Interleaved OFDM

Huyen Le Thi Thanh*, Vu-Duc Ngo†, Minh-Tuan Le‡, Xuan Nam Tran*
*Le Quy Don Technical University, 236 Hoang Quoc Viet, Cau Giay, Ha Noi, Vietnam
†Hanoi University of Science and Technology, Hanoi, Vietnam
‡MobiFone R&D Center, MobiFone Corporation, Hanoi, Vietnam
Email: huyen.ltt@mta.edu.vn, duc.ngovu@hust.edu.vn, tuan.minh@mobifone.vn, namtx@mta.edu.vn

***Abstract*—In this work, a novel index modulation scheme for orthogonal frequency division multiplexing (IM-OFDM), referred to as repeated index modulation with coordinate interleaved OFDM (RIM-CI-OFDM), is proposed to improve the error performance of the conventional IM-OFDM with coordinated interleaving (IM-OFDM-CI) system. Unlike the conventional scheme, RIM-CI-OFDM allows two distinguishable clusters of sub-carriers to employ the same indices of active sub-carriers, while the CI principle is jointly applied to the M-ary data symbols from both of these clusters. As a result, the proposed scheme not only outperforms IM-OFDM-CI in terms of index and M-ary symbol error performances but also provides a better trade-off between the reliability and the spectral efficiency (SE). In addition, our scheme allows the number of active sub-carriers to be any positive integer while it is fixed to an even number in the conventional IM-OFDM-CI. A low complexity maximum likelihood (lowML) detector, which enjoys the optimal error performance as the ML detector at much lower complexity, is also proposed. Finally, simulation results are presented to validate the better performance of the proposed RIM-CI-OFDM and lowML detector in comparison with benchmark schemes.**

***Keywords*—Index modulation, IM-OFDM, coordinate interleaving, ML detection.**

I. Introduction

Orthogonal frequency division multiplexing (OFDM) is known as an effective transmission technique which has high spectral efficiency and robustness against the frequency selectivity of multi-path fading channels. Index modulation is a special type of OFDM, which activates only a subset of sub-carriers for transmission [1].

Different from OFDM, in the index modulated OFDM (IM-OFDM) system, information bits are conveyed by both the M-ary modulated symbols and indices of active sub-carriers. In the original IM-OFDM system, a fixed number of information bits is used to activate the sub-carriers, thus limiting its spectral efficiency and error performance [2]. In order to resolve this limitation, the IM-OFDM with adjusted active sub-carriers was proposed in [1] to attain the trade-off between the spectral efficiency and transmission reliability [1]. In order to improve the spectral efficiency, the authors in [3] proposed the so-called IM-OFDM-I/Q scheme which performs IM jointly on both the in-phase and quadrature components of complex data symbols. In another effort, the dual-mode OFDM (DM-OFDM) solution introduced in [4] exploits inactive sub-carriers to convey additional data bits. Different signal constellations were used for data symbols transmitted over the active and in-active sub-carriers. Developing this idea, the multi-mode IM-OFDM (MM-IM-OFDM) was proposed in [5]. This scheme activates all sub-carriers and employs the permutation of transmission modes to carry additional data bits, thus further increases the spectral efficiency.

In order to cope with the transmission reliability issue, a sub-carrier interleaving solution was proposed in [6] to increase the Euclidean distance between the M-ary modulated symbols. In [7], the interleaved sub-carrier grouping and the achievable rate of IM-OFDM were investigated.

Recently, various efforts have also paid to analyze performance of IM-OFDM systems. A tight bound for the bit error rate (BER) of IM-OFDM was successfully derived in [8]. In [9], the authors evaluated the outage performance of the IM-OFDM system over two-way diffused-power fading channels. The error performance of IM-OFDM and IM-OFDM using greedy detection under imperfect channel state information (CSI) were investigated in [10] and [11], respectively.

In an effort to attain transmit diversity gain, the coordinate interleaved IM-OFDM scheme in [12] distributed the real and imaginary components of transmit complex symbols over distinctive sub-carriers. The paper [13] introduced an IM-OFDM scheme with transmit diversity, which utilized multiple signal constellations to carry the same data bits over the active sub-carriers. In the recent work [14], the coded IM-OFDM with transmit diversity (TD-IM-OFDM) was proposed to increase the reliability for index detection. To further improve the diversity gain and error performance, the IM-OFDM concept was extended to MIMO systems in [15], [16]. In order to reduce complexity while still improving the diversity gain of IM-OFDM, the study in [17] introduced the IM-OFDM with greedy detection and diversity reception. Its BER performance under imperfect CSI was analyzed in [18]. The repeated IM-OFDM with transmit diversity and the closed-form expressions for its symbol error probability were presented in [19]. More recently, in [20], [21], different spreading matrices are utilized to increase the diversity gain of the conventional IM-OFDM.

In this paper, aiming at improving the error performance of the conventional IM-OFDM-CI system, we propose a repeated index modulation with coordinate interleaved OFDM (RIM-CI-OFDM) scheme. In our scheme, coordinate interleaving is simultaneously applied to the M-ary modulated symbols in two different clusters. In addition, these distinct clusters repeatedly utilize the same set of active sub-carrier indices. Combining coordinate interleaving and the index repetition allows RIM-CI-OFDM to attain better index detection and the M-ary modulated symbol error performance over the conventional IM-OFDM-CI system, even at the same spectral efficiency. Furthermore, while IM-OFDM-CI requires an even number of active sub-carriers, our proposed scheme can

978-1-5386-7983-8/18/$31.00 ©2018 IEEE

activate an arbitrary number of sub-carriers and thus is more flexible in terms of achieving reliability and spectral efficiency. We also propose a low-complexity ML detector that attains the equivalent error performance of the optimal ML detector.

The remainder of this paper is organized as follows. Section II describes the system model of the proposed RIM-CI-OFDM. The low-complexity ML detector is introduced in Section III. Section IV presents the simulation results and discussions. Finally, the conclusion is given in Section IV.

Notation: Vectors and matrices are denoted by bold letters. $C(\ ,\ )$ and $\lfloor\cdot\rfloor$ present the binomial coefficient and the floor function, respectively. $\mathbb{E}\{\cdot\}$ is the expectation operation. $(\cdot)^R$ and $(\cdot)^I$ denote the real and imaginary parts of a complex number, respectively.

II. System Model

Consider a RIM-CI-OFDM system as illustrated in Fig. 1. There are total N_F sub-carriers available to transmit m information bits. The system is partitioned into G sub-blocks of N_G sub-carriers and p bits, i.e., $N_F = GN_G$ and $m = Gp$. Then, each sub-block is split into two clusters of N sub-carriers, i.e., $N_G = 2N$. Since the operation in each sub-block is independent, without loss of generality, we investigate only one instead of G sub-blocks.

For each sub-block transmission, $p_1 = \lfloor \log_2 (C(N,K)) \rfloor$ bits are sent to an index selector to determine K out of N sub-carriers using either a look-up table (LUT) or the combinatorial method [1]. Similar to the IM-OFDM system, an additional number of information bits is transferred through the indices of active sub-carriers. The inactive sub-carriers are idle. The output of the index selector is a set of activated sub-carrier indices θ, i.e., $\theta = \{\alpha_1, \ldots, \alpha_K\}$, where $\alpha_k \in \{1, \ldots, N\}$ and $k = \{1, \ldots, K\}$. Let $\mathcal{I}$ denote the set of possible active indices. For the given values of N and K, there are total $c = 2^{\lfloor \log_2 C(N,K) \rfloor}$ active index combinations. Unlike the conventional IM-OFDM-CI, RIM-CI-OFDM employs the same set of active sub-carrier indices θ for two clusters in one sub-block as shown in Fig. 1. It is noteworthy that such the index repetition can improve the index error probability (IEP) over the conventional scheme at the cost of spectral efficiency.

The remaining bits are equally separated into two clusters of $p_2 = K\log_2 M$ bits. Thanks to the index repetition between two clusters, we can jointly apply the coordinate interleaving technique to M-ary modulated symbols from two distinguishable clusters. For every cluster, $p_2 = K\log_2 M$ bits are mapped into a vector of K M-ary modulated symbols $\mathbf{s}_i \in \mathbb{C}^{K\times 1}$, for $i = 1, 2$. Let $\mathbf{s}_1 = [a_1\ a_2\ \ldots\ a_K]^T$ and $\mathbf{s}_2 = [b_1\ b_2\ \ldots\ b_K]^T$. Prior to the coordinate interleaving, all M-ary modulated symbols in $\mathbf{s}_i$ are rotated by an angle ϕ which is defined based on the M-ary modulation type. Let $\mathcal{S}^\phi$ denote the rotated constellation. The values of ϕ can be selected by the computer search method [12]. For example, the QAM constellation size $M = \{2, 4, 16, 64\}$, rotation angles are respectively given by $\phi = \{45°, 15°, 8.5°, 4.5°\}$. After coordinate interleaving between the symbols in $\mathbf{s}_1$ and $\mathbf{s}_2$ from different clusters, the symbol vectors in each cluster, $\tilde{\mathbf{s}_\mathbf{i}} \in \mathbb{C}^{K\times 1}$, are obtained as

$$\tilde{\mathbf{s}}_1 = \begin{bmatrix} c_{1,1} \\ c_{1,2} \\ \vdots \\ c_{1,K-1} \\ c_{1,K} \end{bmatrix} = \begin{bmatrix} a_1^R + \jmath b_1^I \\ a_2^R + \jmath b_2^I \\ \vdots \\ a_{K-1}^R + \jmath b_{K-1}^I \\ a_K^R + \jmath b_K^I \end{bmatrix} \tag{1}$$

$$\tilde{\mathbf{s}}_2 = \begin{bmatrix} c_{2,1} \\ c_{2,2} \\ \vdots \\ c_{2,K-1} \\ c_{2,K} \end{bmatrix} = \begin{bmatrix} b_1^R + \jmath\jmath a_1^I \\ b_2^R + \jmath a_2^I \\ \vdots \\ b_{K-1}^R + \jmath a_{K-1}^I \\ b_K^R + \jmath a_K^I \end{bmatrix}. \tag{2}$$

where $\jmath = \sqrt{-1}$. Using $\tilde{\mathbf{s}}_i$ and θ, the transmitted codeword over N sub-carriers $\mathbf{x}_i = [x_{i1}, \ldots, x_{iN}]^T$ is generated. Since only K out of N sub-carriers are activated, K symbols corresponding to the active sub-carriers are nonzero, i.e., $x_{i\alpha_k} = c_{i,k}$ when $\alpha_k \in \theta$, and $x_{i\alpha_k} = 0$ when $\alpha_k \notin \theta$, where $\alpha_k = \{1, \ldots, N\}$, $k = \{1, \ldots, K\}$, $i = 1, 2$. An example of a lookup table to determine the transmitted codewords in each cluster when $N = 4$, $K = 2$, $p_1 = 2$ is presented in Table I. It is clear that for each data symbol within a cluster, its real and imaginary components are transferred over different sub-carriers. In addition, combining the index repetition and the joint coordinate interleaving method allows RIM-CI-OFDM to activate an arbitrary number of sub-carriers, leading to higher flexibility in terms of the transmission reliability and spectral efficiency compared with the conventional IM-OFDM-CI.

The OFDM sub-block creator takes into account $\mathbf{x}_1$ and $\mathbf{x}_2$ to generate the transmitted signal per sub-block that is given by $\mathbf{x} = \begin{bmatrix}\mathbf{x}_1^T\ \mathbf{x}_2^T\end{bmatrix}^T$. For each RIM-IM-OFDM sub-block, the received signal in frequency domain can be expressed as

$$\mathbf{y} = \mathbf{H}\mathbf{x} + \mathbf{n}, \tag{3}$$

where $\mathbf{y} = [\mathbf{y}_1\ \mathbf{y}_2]^T$, $\mathbf{H} = \begin{bmatrix} \mathbf{H}_1 & \mathbf{0} \\ \mathbf{0} & \mathbf{H}_2 \end{bmatrix}$ and $\mathbf{n} = \begin{bmatrix}\mathbf{n}_1^T\ \mathbf{n}_2^T\end{bmatrix}^T$. The components $\mathbf{y}_i = [y_{i1}, \ldots, y_{iN}]$ and $\mathbf{H}_i = \text{diag}\{h_{i1}, \ldots, h_{iN}\}$, for $i = 1, 2$, are the received signal and the Rayleigh channel matrix of the i-th cluster, respectively. The noise component vector is given by $\mathbf{n}_i = [n_{i1}, \ldots, n_{iN}]^T$. On each sub-channel α, the channel coefficient $h_{i\alpha}$ and noise $n_{i\alpha}$ are the complex Gaussian random variables that respectively follow $\mathcal{CN}(0, 1)$ and $\mathcal{CN}(0, N_0)$ distributions, where N_0 represents the noise variance. The average signal to noise ratio (SNR) per sub-carrier is determined by $\bar{\gamma} = \omega E_s/N_0$, where ωE_s denotes the average transmit power per M-ary modulated symbol, i.e., $\mathbb{E}\{|s|^2\} = \omega E_s$. The power allocation factor and the average power per sub-carrier are respectively denoted by $\omega = N/K$ and E_s.

Consequently, the total number of information bits that are transmitted per sub-block is $p = p_1 + 2p_2$ bits. As a result, the spectral efficiency of the RIM-CI-OFDM system is given by

$$\eta = \frac{\lfloor \log_2 (C(N,K)) \rfloor + 2K\log_2 M}{2N} \quad [\text{bits/s/Hz}]. \tag{4}$$

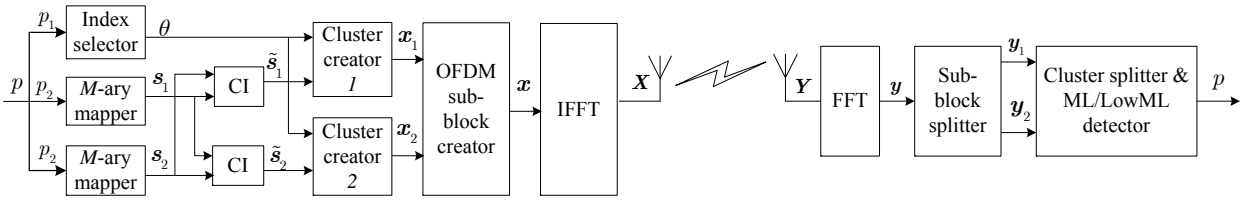

Fig. 1. Block diagram of the RIM-CI-OFDM system with two clusters per sub-block.

TABLE I. EXAMPLE OF LUT WITH $N = 4$, $K = 2$, $p_1 = 2$.

p_1	θ	$\mathbf{x}_1^T$	$\mathbf{x}_2^T$
00	$[1, 2]$	$\begin{bmatrix} a_1^R + \jmath b_1^I & a_2^R + \jmath b_2^I & 0 & 0 \end{bmatrix}$	$\begin{bmatrix} b_1^R + \jmath a_1^I & b_2^R + \jmath a_2^I & 0 & 0 \end{bmatrix}$
01	$[2, 3]$	$\begin{bmatrix} 0 & a_1^R + \jmath b_1^I & a_2^R + \jmath b_2^I & 0 \end{bmatrix}$	$\begin{bmatrix} 0 & b_1^R + \jmath a_1^I & b_2^R + \jmath a_2^I & 0 \end{bmatrix}$
10	$[2, 4]$	$\begin{bmatrix} 0 & a_1^R + \jmath b_1^I & 0 & a_2^R + \jmath b_2^I \end{bmatrix}$	$\begin{bmatrix} 0 & b_1^R + \jmath a_1^I & 0 & b_2^R + \jmath a_2^I \end{bmatrix}$
11	$[1, 3]$	$\begin{bmatrix} a_1^R + \jmath b_1^I & 0 & a_2^R + \jmath b_2^I & 0 \end{bmatrix}$	$\begin{bmatrix} b_1^R + \jmath a_1^I & 0 & b_2^R + \jmath a_2^I & 0 \end{bmatrix}$

In order to estimate the transmitted signal, the receiver utilizes an ML detector to jointly detect the indices of active sub-carriers and corresponding M-ary modulated symbols for both clusters. The ML detector selects the codeword that minimizes the decision metric as follows

$$\left(\hat{\theta}, \hat{\mathbf{s}}_1, \hat{\mathbf{s}}_2\right) = \arg\min_{\theta, \mathbf{s}_1, \mathbf{s}_2} \|\mathbf{y} - \mathbf{H}\mathbf{x}\|^2. \tag{5}$$

It can be seen that the complexity of the ML detector is $\sim \mathcal{O}\left(2^{p_1} M^{2K}\right)$ which exponentially increases with M. In order to reduce the computational complexity of the ML, we propose a low-complexity ML detector in the next section.

III. LOW-COMPLEXITY ML DETECTOR

For each possible combination of $\theta = \{\alpha_1, \ldots, \alpha_K\}$, which is represented by θ_j, where $j = 1, \ldots, 2^{p_1}$, $\theta_j \in \mathcal{I}$, we can express the received signal for sub-carrier $\alpha_k \in \theta_j$, where $k = 1, ..., K$, as follows

$$\begin{bmatrix} y_{1\alpha_k}^R \\ y_{1\alpha_k}^I \\ y_{2\alpha_k}^R \\ y_{2\alpha_k}^I \end{bmatrix}_j = \begin{bmatrix} h_{1\alpha_k}^R & 0 & 0 & -h_{1\alpha_k}^I \\ h_{1\alpha_k}^I & 0 & 0 & h_{1\alpha_k}^R \\ 0 & -h_{2\alpha_k}^I & h_{2\alpha_k}^R & 0 \\ 0 & h_{2\alpha_k}^R & h_{2\alpha_k}^I & 0 \end{bmatrix}_j \times \begin{bmatrix} a_k^R \\ a_k^I \\ b_k^R \\ b_k^I \end{bmatrix} + \begin{bmatrix} n_{1\alpha_k}^R \\ n_{1\alpha_k}^I \\ n_{2\alpha_k}^R \\ n_{2\alpha_k}^I \end{bmatrix}_j \tag{6}$$

Equation (6) can be rewritten as

$$\left(\bar{\mathbf{y}}_{\alpha_k}\right)_j = \left(\bar{\mathbf{H}}_{\alpha_k}\right)_j \bar{\mathbf{s}}_k + \left(\bar{\mathbf{n}}_{\alpha_k}\right)_j, \tag{7}$$

where $\left(\bar{\mathbf{H}}_{\alpha_k}\right)_j = \left[\left(\bar{\mathbf{H}}_{1\alpha_k}\right)_j \ \left(\bar{\mathbf{H}}_{2\alpha_k}\right)_j\right]^T$, $\left(\bar{\mathbf{H}}_{1\alpha_k}\right)_j$ and $\left(\bar{\mathbf{H}}_{2\alpha_k}\right)_j$ are respectively given by

$$\left(\bar{\mathbf{H}}_{1\alpha_k}\right)_j = \begin{bmatrix} h_{1\alpha_k}^R & 0 \\ h_{1\alpha_k}^I & 0 \\ 0 & -h_{2\alpha_k}^I \\ 0 & h_{2\alpha_k}^R \end{bmatrix}_j, \quad \left(\bar{\mathbf{H}}_{2\alpha_k}\right)_j = \begin{bmatrix} 0 & -h_{1\alpha_k}^I \\ 0 & h_{1\alpha_k}^R \\ h_{2\alpha_k}^R & 0 \\ h_{2\alpha_k}^I & 0 \end{bmatrix}_j. \tag{8}$$

Since the orthogonal property exists for the columns of channel matrix $\left(\bar{\mathbf{H}}_{\alpha_k}\right)_j$, the single-symbol ML detector can be used to independently estimate $\hat{a}_{k,j}$ and $\hat{b}_{k,j}$ as follows

$$\begin{aligned} \hat{a}_{k,j} &= \arg\min_{a_k \in \mathcal{S}_\phi} \left\| \left(\bar{\mathbf{y}}_{\alpha_k}\right)_j - \left(\bar{\mathbf{H}}_{1\alpha_k}\right)_j \left[a_k^R \ a_k^I\right]^T \right\|^2, \\ \hat{b}_{k,j} &= \arg\min_{b_k \in \mathcal{S}_\phi} \left\| \left(\bar{\mathbf{y}}_{\alpha_k}\right)_j - \left(\bar{\mathbf{H}}_{2\alpha_k}\right)_j \left[b_k^R \ b_k^I\right]^T \right\|^2. \end{aligned} \tag{9}$$

Upon having the results from (9), the coordinate interleaving principle is applied to each pair of $\left(\hat{a}_{k,j}, \hat{b}_{k,j}\right)$ to create $\tilde{\mathbf{s}}_1, \tilde{\mathbf{s}}_2$ as in (1) and (2). Then, $\tilde{\mathbf{s}}_1, \tilde{\mathbf{s}}_2$ and θ_j are combined to generate $N \times 1$ symbol vectors $\hat{\mathbf{x}}_{i,j}$. The lowML detector will make a final decision on the indices of active sub-carriers which corresponds to the best estimated symbols by

$$\hat{j} = \arg\min_j \{D_j\}, \tag{10}$$

where $D_j = \|\mathbf{y}_1 - \mathbf{H}_1 \hat{\mathbf{x}}_{1,j}\|^2 + \|\mathbf{y}_2 - \mathbf{H}_2 \hat{\mathbf{x}}_{2,j}\|^2$. Using $\hat{j}$ the estimated set of active sub-carrier indices is given by $\hat{\theta} = \theta_{\hat{j}}$. The M-ary modulated symbols of both clusters are then

detected as follows

$$\hat{a}_k = \hat{a}_{k,\hat{j}}, \quad \hat{b}_k = \hat{b}_{k,\hat{j}}. \tag{11}$$

Based on estimated symbols $\hat{a}_k$ and $\hat{b}_k$, where $k = 1, \ldots, K$, the symbol vectors for each cluster are obtained by

$$\hat{\mathbf{s}}_1 = \left[\hat{a}_1 \ \hat{a}_2 \ \ldots \ \hat{a}_K\right]^T, \quad \hat{\mathbf{s}}_2 = \left[\hat{b}_1 \ \hat{b}_2 \ \ldots \ \hat{b}_K\right]^T. \tag{12}$$

The low-complexity ML detection algorithm is summarized in Algorithm 1. It can be seen that unlike the ML detector, the proposed lowML detector has the computational complexity of $\sim \mathcal{O}\left(2^{p_1} MK\right)$, which linearly increases with M.

Algorithm 1 Low-complexity ML detection algorithm

Input: $\mathbf{y}_1$, $\mathbf{y}_2$, $\mathbf{H}_1$, $\mathbf{H}_2$, $\mathcal{S}^{\phi}$, $\mathcal{I}$.
Output: $\hat{\theta}$, $\hat{\mathbf{s}}_1$, $\hat{\mathbf{s}}_2$.

for $j = 1$ **to** 2^{p_1} **do**
  for $k = 1$ **to** K **do**
    Define $\left(\bar{\mathbf{y}}_{\alpha_k}\right)_j = \left[y^R_{1\alpha_k} \ y^I_{1\alpha_k} \ y^R_{2\alpha_k} \ y^I_{2\alpha_k}\right]^T_j$.
    Calculate $\left(\bar{\mathbf{H}}_{1\alpha_k}\right)_j$, $\left(\bar{\mathbf{H}}_{2\alpha_k}\right)_j$ as in (8).
    Estimate $\hat{a}_{k,j}$ and $\hat{b}_{k,j}$ according to (9).
  end for
  From $\hat{a}_{k,j}$ and $\hat{b}_{k,j}$, create $\tilde{\mathbf{s}}_{1,j}$, $\tilde{\mathbf{s}}_{2,j}$ as in (1), (2).
  Combine $\tilde{\mathbf{s}}_{1,j}, \tilde{\mathbf{s}}_{2,j}$ and θ_j to generate $\hat{\mathbf{x}}_{1,j}$, $\hat{\mathbf{x}}_{2,j}$.
  Compute $D_j = \sum_{i=1}^{2} \|\mathbf{y}_i - \mathbf{H}_i \hat{\mathbf{x}}_{i,j}\|^2$, for $i = 1, 2$.
end for
Estimate $\hat{j} = \arg \min_{j=1,\ldots,2^{p_1}} D_j$
Generate $\hat{\theta} = \theta_{\hat{j}}$, $\hat{a}_k = \hat{a}_{k,\hat{j}}$, $\hat{b}_k = \hat{b}_{k,\hat{j}}$.
  $\hat{\mathbf{s}}_1$, $\hat{\mathbf{s}}_2$ as in (12).
Output: $\hat{\theta}$, $\hat{\mathbf{s}}_1$, $\hat{\mathbf{s}}_2$.

IV. Simulation Results and Discussions

This section presents simulation results of the proposed RIM-CI-OFDM and lowML detector. It is assumed that the channel over each sub-carrier is flat Rayleigh fading. For comparison, IM-OFDM [1] and IM-OFDM-CI [12] are selected as reference schemes. A system with total N sub-carriers, K active sub-carriers and signal constellation size M is referred to as (N, K, M).

Fig. 2 compares the index error probability (IEP) performance of the proposed RIM-CI-OFDM, the conventional IM-OFDM and the IM-OFDM-CI system when $N = 4$, $K = \{2, 3\}$, $M = 2$. It can be seen from the figure that the proposed scheme achieves significantly better IEP performance than the two reference systems. Particularly, at the IEP of 10^{-4}, the proposed scheme attains SNR gains of 8 dB and 5.5 dB over the IM-OFDM and IM-OFDM-CI systems, respectively. Since the proposed scheme jointly uses index repetition and coordinate interleaving, it can achieve better diversity gain in the index domain than IM-OFDM and IM-OFDM-CI.

Fig. 3 depicts the BER comparison among RIM-CI-OFDM, IM-OFDM and IM-OFDM-CI systems when $M = 2$, $N = 4$, $K = \{2, 3\}$. As seen from this figure, at the same spectral efficiency and BER of 10^{-4}, the proposed scheme provides an SNR gain of about 10 dB and 2 dB over the two benchmark

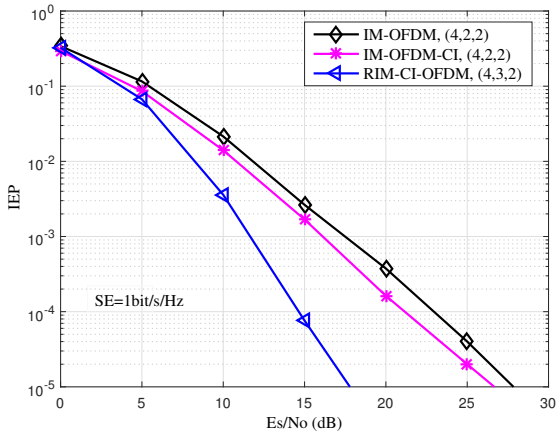

Fig. 2. Index error performance of the proposed RIM-CI-OFDM compared with the conventional IM-OFDM and IM-OFDM-CI system, at the spectral efficiency (SE) of 1 bit/s/Hz, $M = 2$, $N = 4$, $K = \{2, 3\}$.

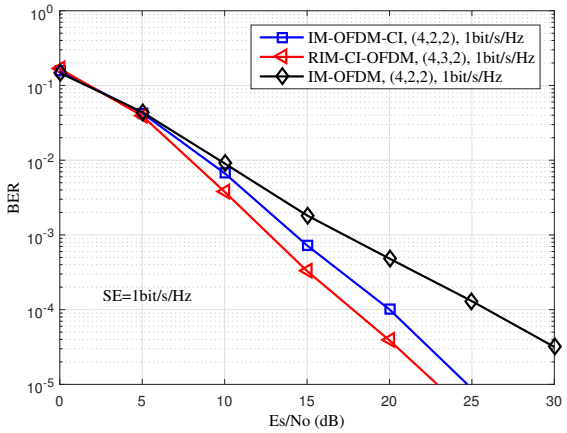

Fig. 3. The BER performance of the RIM-CI-OFDM in comparison with the classical IM-OFDM and CI-IM-OFDM at the spectral efficiency of 1 bit/s/Hz when $M = 2$, $N = 4$, $K = \{2, 3\}$.

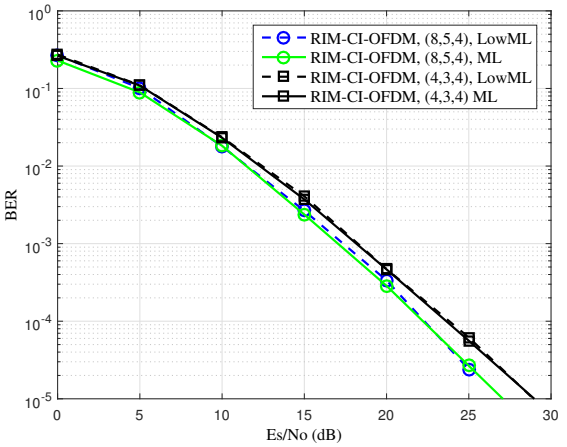

Fig. 4. BER performance of the RIM-CI-OFDM scheme when using ML and lowML with $M = 4$, $N = \{4, 8\}$, $K = \{3, 5\}$.

systems. This is because in RIM-CI-OFDM, the IEP improvement, as shown in Fig. 2, allows for reduction in errors of the M-ary modulated symbol detection, leading to improve the overall error performance compared with benchmark schemes.

Comparison of the BER performance between ML and lowML detectors when $M = 4$, $N = \{4, 8\}$, $K = \{3, 5\}$ is shown in Fig. 4. It can be observed from Fig. 4 that the proposed lowML detector can achieve the same error performance as ML, while having much lower complexity compared with ML.

V. Conclusion

This paper has proposed a novel IM-OFDM scheme, named as RIM-CI-OFDM, which provides higher reliability and flexibility than the conventional IM-OFDM-CI system. By using the same set of active sub-carrier indices in two distinguishable clusters and jointly applying the coordinate interleaving to M-ary modulated symbols in them, the proposed RIM-CI-OFDM scheme can reduce both the index and symbol error probabilities while having higher flexibility in terms of the transmission reliability and the spectral efficiency. The proposed low-complexity ML detector allows the system to reduce further computational complexity while enjoying the optimal BER performance. Simulation results clearly confirmed the advantages of the proposed scheme over the IM-OFDM and IM-OFDM-CI system.

References

[1] E. Başar, Ü. Aygölü, E. Panayırcı, and H. V. Poor, "Orthogonal frequency division multiplexing with index modulation," *IEEE Trans. Signal Process.*, vol. 61, no. 22, pp. 5536–5549, Aug. 2013.

[2] R. Abu-Alhiga and H. Haas, "Subcarrier-index modulation OFDM," in *IEEE Int. Sym. Pers., Indoor and Mobile Radio Commun.* IEEE, Sep. 2009, pp. 177–181.

[3] B. Zheng, F. Chen, M. Wen, F. Ji, H. Yu, and Y. Liu, "Low-complexity ML detector and performance analysis for OFDM with in-phase/quadrature index modulation," *IEEE Commun. Lett*, vol. 19, no. 11, pp. 1893–1896, Nov. 2015.

[4] T. Mao, Z. Wang, Q. Wang, S. Chen, and L. Hanzo, "Dual-mode index modulation aided OFDM," *IEEE Access*, vol. 5, pp. 50–60, Feb. 2017.

[5] M. Wen, E. Basar, Q. Li, B. Zheng, and M. Zhang, "Multiple-mode orthogonal frequency division multiplexing with index modulation," *IEEE Trans. Commun.*, vol. 65, no. 9, pp. 3892–3906, May. 2017.

[6] Y. Xiao, S. Wang, L. Dan, X. Lei, P. Yang, and W. Xiang, "OFDM with interleaved subcarrier-index modulation," *IEEE Commun. Lett.*, vol. 18, no. 8, pp. 1447–1450, Jun. 2014.

[7] M. Wen, X. Cheng, M. Ma, B. Jiao, and H. V. Poor, "On the achievable rate of OFDM with index modulation," *IEEE Trans. Signal Process.*, vol. 64, no. 8, pp. 1919–1932, Apr. 2016.

[8] Y. Ko, "A tight upper bound on bit error rate of joint OFDM and multi-carrier index keying," *IEEE Commun. Lett.*, vol. 18, no. 10, pp. 1763–1766, Oct. 2014.

[9] T. Van Luong and Y. Ko, "Symbol Error Outage Performance Analysis of MCIK-OFDM over Complex TWDP Fading," in *2017 European Wireless Conf.* VDE, May 2017, pp. 1–5.

[10] ——, "A Tight Bound on BER of MCIK-OFDM With Greedy Detection and Imperfect CSI," *IEEE Commun. Lett.*, vol. 21, no. 12, pp. 2594–2597, Aug. 2017.

[11] ——, "Impact of CSI uncertainty on MCIK-OFDM: Tight closed-form symbol error probability analysis," *IEEE Trans. Veh. Technol.*, vol. 67, no. 2, pp. 1272–1279, Feb. 2018.

[12] E. Başar, "OFDM with index modulation using coordinate interleaving," *IEEE Wireless Commun. Lett.*, vol. 4, no. 4, pp. 381–384, Aug. 2015.

[13] J. Zheng and R. Chen, "Achieving transmit diversity in OFDM-IM by utilizing multiple signal constellations," *IEEE Access*, vol. 5, pp. 8978–8988, Aug. 2017.

[14] J. Choi, "Coded OFDM-IM with transmit diversity," *IEEE Trans. Commun.*, vol. 65, no. 7, pp. 3164–3171, Jul. 2017.

[15] E. Başar, "Multiple-input multiple-output OFDM with index modulation," *IEEE Signal Process. Lett.*, vol. 22, no. 12, pp. 2259–2263, Dec. 2015.

[16] B. Zheng, M. Wen, E. Basar, and F. Chen, "Multiple-input multiple-output OFDM with index modulation: Low-complexity detector design," *IEEE Trans. Signal Process.*, vol. 65, no. 11, pp. 2758–2772, Jun. 2017.

[17] J. Crawford, E. Chatziantoniou, and Y. Ko, "On the SEP analysis of OFDM index modulation with hybrid low complexity greedy detection and diversity reception," *IEEE Trans. Veh. Technol.*, vol. 66, no. 9, pp. 8103–8118, Apr. 2017.

[18] T. Van Luong and Y. Ko, "The BER Analysis of MRC-aided Greedy Detection for OFDM-IM in Presence of Uncertain CSI," *IEEE Wireless Commun. Lett.*, Jan. 2018.

[19] T. Van Luong, Y. Ko, and J. Choi, "Repeated MCIK-OFDM With Enhanced Transmit Diversity Under CSI Uncertainty," *IEEE Trans. Wireless Commun.*, vol. 17, no. 6, pp. 4079–4088, Jun. 2018.

[20] T. V. Luong, Y. Ko, and J. Choi, "Precoding for spread OFDM IM," in *Proc. IEEE 87th Veh. Technol. Conf. (VTC Spring)*, 2018, pp. 1–5.

[21] T. V. Luong and Y. Ko, "Spread OFDM-IM with precoding matrix and low-complexity detection designs," *IEEE Trans. Veh. Technol.*, to be published.